



Published in final edited form as:

Bioorg Med Chem. 2013 November 01; 21(21): 6657–6664. doi:10.1016/j.bmc.2013.08.015.

TRPV1 antagonist with high analgesic efficacy: 2-Thio pyridine C-region analogues of 2-(3-fluoro-4-methylsulfonylaminophenyl) propanamides

Tae-Hwan Ha^a, HyungChul Ryu^a, Sung-Eun Kim^a, Ho Shin Kim^a, Jihyae Ann^a, Phuong-Thao Tran^a, Van-Hai Hoang^a, Karam Son^b, Minghua Cui^b, Sun Choi^b, Peter M. Blumberg^c, Robert Frank^d, Gregor Bahrenberg^d, Klaus Schiene^d, Thomas Christoph^d, Sven Frommann^d, Jeewoo Lee^{a,*}

^aLaboratory of Medicinal Chemistry, Research Institute of Pharmaceutical Sciences, College of Pharmacy, Seoul National University, Seoul 151-742, Republic of Korea

^bNational Leading Research Lab (NLRL) of Molecular Modeling & Drug Design, College of Pharmacy, Division of Life and Pharmaceutical Sciences, and Global Top5 Research Program, Ewha Womans University, Seoul 120-750, Republic of Korea

^cLaboratory of Cancer Biology and Genetics, Center for Cancer Research, National Cancer Institute, NIH, Bethesda, MD 20892, USA

^dGrunenthal Innovation, Grunenthal GmbH, D-52078 Aachen, Germany

Abstract

A series of 2-thio pyridine C-region analogues of 2-(3-fluoro-4-methylsulfonylaminophenyl)propanamides were investigated as *h*TRPV1 antagonists. Among them, compound **24S** showed stereospecific and excellent TRPV1 antagonism of capsaicin-induced activation. Further, it demonstrated strong anti-allodynic in a rat neuropathic pain model. Consistent with its action in vitro being through TRPV1, compound **24S** blocked capsaicin-induced hypothermia in mice. Docking analysis of **24S** with our *h*TRPV1 homology model was performed to identify its binding mode.

Keywords

TRPV1 antagonists; Analgesic; Capsaicin; Resiniferatoxin

1. Introduction

The transient receptor potential V1 (TRPV1) receptor is a molecular integrator of nociceptive stimuli predominantly expressed on sensory neurons.¹ It is activated by multiple endogenous agonists including protons,² noxious heat,³ and inflammatory lipid mediators^{4,5} as well as by natural products such as capsaicin (CAP)⁶ and resiniferatoxin (RTX).⁷ The pharmacological blockade of TRPV1, by inhibiting the transmission of nociceptive signaling

*Corresponding author. Tel.: +82 2 880 7846; fax: +82 2 888 0649. jeewoo@snu.ac.kr (J. Lee).

from the periphery to the CNS, provides a promising strategy for the development of novel analgesics.⁸ Since the molecular cloning of TRPV1 in 1997,³ a massive effort to identify potent and selective TRPV1 antagonists has been made to develop clinical candidates as novel analgesic and antiinflammatory agents, particularly for neuropathic pain. The clinical development and therapeutic potential of TRPV1 antagonists have been extensively reviewed.⁹⁻¹⁵

Recently, we reported that compound **2** showed highly selective and potent antagonism of TRPV1 with $K_{i(\text{CAP})} = 0.2$ nM and $\text{IC}_{50(\text{pH})} = 6.3$ nM, being thus approximately 100-fold and 20-fold better than prototype **1**¹⁶ for CAP and pH antagonism, respectively (Fig. 1).¹⁷ In addition, compound **2** demonstrated strong anti-allodynic activity in a neuropathic pain model with almost no off target effects and blocked capsaicin-induced hypothermia in mice. The structural analysis indicated that the enhanced potency of **2** was attributed to the additional 4-methylpiperidine moiety in **2** compared to **1**, which provided a new hydrophobic interaction with the receptor. Indeed, the docking analysis using our hTRPV1 homology model indicated that the 4-methylpiperidinyl group in the C-region of **2** made additional hydrophobic interactions with the hydrophobic region composed of Met514 and Leu515, an interaction not occurring with **1**.¹⁸

In order to further optimize the 2-substituent in the *N*-(6-trifluoromethyl-pyridin-3-ylmethyl) C-region, we have investigated the structure–activity relationship of 2-thio derivatives (Fig. 2) as hTRPV1 antagonists. With a selected potent antagonist in the series, we further characterized target engagement by assessing its potential to inhibit capsaicin-induced hypothermia and its anti-allodynic activity in animal models and performed molecular modeling with our hTRPV1 homology model.

2. Result and discussion

2.1. Chemistry

The key intermediate of the C-region **3** was prepared as described in the previous report.¹⁷ A library of thiols were reacted with **3** to afford 2-thio substituted pyridines **4** and then their nitrile groups were reduced to yield the corresponding primary amines **5**. The amines were coupled with racemic or chiral 2-(3-fluoro-4-methylsulfonylaminophenyl) propanamide **6** to provide the final compounds **7–39**, respectively (Scheme 1).

2.2. Structure-activity relationship (SAR) analysis

The synthesized TRPV1 ligands were evaluated in vitro for antagonism as measured by inhibition of activation by capsaicin (CAP) and pH as indicated. The assays were conducted using a fluorometric imaging plate reader (FLIPR) with human TRPV1 heterologously expressed in Chinese hamster ovary (CHO) cells.¹⁷ The results are summarized in Tables 1-3, together with the potencies of the previously reported antagonists **1** and **2**.^{16,17}

To investigate the SAR for 2-thio derivatives of the pyridine C-region, we began with the 2-alkylthio derivatives (Table 1). Previous SAR analysis with a series of 2-alkyloxy derivatives indicated that the 2-butyloxy group was among the most optimal with low lipophilicity and potent antagonism.¹⁸ The 2-butythio derivative **7** likewise proved to be a potent antagonist

with $K_{i(\text{CAP})} = 0.7$ nM and $\text{IC}_{50(\text{pH})} = 40.4$ nM but was nonetheless ca. twofold and fivefold less potent than the racemate of **2** ($K_{i(\text{CAP})} = 0.3$ nM and $\text{IC}_{50(\text{pH})} = 8.4$ nM), respectively. As the number of carbons in the chain further increased, antagonistic activity decreased as seen with **8** and **9**. The branched derivative **10** showed better antagonism than the corresponding straight derivative **8** by threefold. With potent antagonist **7**, we explored the SAR at its terminal position by introducing different types of groups. The lipophilic moieties such as trifluoromethyl (**11**), bromo (**12**) and phenoxy (**13**) caused a reduction in activity compared to **7** but still provided good antagonism. The polar moieties such as hydroxyl (**14**) and dimethylamine (**15**) led to a further reduction in activity. However, the introduction of cyclic amines such as pyrrolidine (**16**), piperidine (**17**) and 4-methylpiperidine (**18**) produced reasonable antagonism in the range of $K_{i(\text{CAP})} = 2\text{--}3$ nM. The morpholine derivative (**19**) showed weak antagonism due to its polar oxygen, as was the case with **14**. The carboxylate moieties (**20–22**) similarly reduced the potency because of their polarity. The SAR analysis in this series of 2-alkylthio groups indicated that the number of 4 carbons (**7**) appeared to be optimal for antagonism, as had been observed for the 2-alkyloxy groups, and the incorporation of any moiety at the terminus of the 2-alkylthio group led to a reduction in potency.

Next, the SAR of 2-cycloalkylthio derivatives was investigated (Table 2). 2-Cyclopentylthio (**23**) and 2-cyclohexylthio (**24**) analogues exhibited potent antagonism with $K_{i(\text{CAP})} = 1.2$ and 0.9 nM, respectively, which were two and fourfold better than the corresponding acyclic 2-alkylthio derivatives **8** and **9**. The result was contrary to that of the 2-alkyloxy and 2-cycloalkyloxy derivatives and the comparison will be discussed in detail in Table 4. The two stereoisomers of **24** showed stereospecific antagonism, as previously reported,¹⁹ in which eutomer **24S** proved to have excellent antagonism with $K_{i(\text{CAP})} = 0.4$ nM. To examine the effect of substituents on potent antagonist **24**, its derivatives were further investigated. The sulfur oxidation of **24**, providing sulfoxide **25** and sulfone **26**, led to a dramatic loss of activity. Whereas the 4-methyl group in **27** enhanced antagonistic potency by twofold, the 2-methyl group in **28** reduced potency by twofold compared to **24**, respectively. The 4-ethyl derivative **29** showed similar activity to that of the parent **24**, while the 4-*t*-butyl group caused a slight decrease of activity. The 2-cyclohexylmethylthio derivative **31**, the one carbon elongated product of **24**, was 2.5-fold less potent than **24**. The SAR analysis in this series of 2-cycloalkylthio groups indicated that the 2-cyclohexylthio derivative **24** appeared to be optimal for antagonism and the 4-methyl and 4-ethyl groups on the ring were tolerable for potency.

Next, we sought to evaluate the SAR of 2-benzylthio and 2-arylmethylthio derivatives since previous SAR analysis in a series of 2-alkyloxy derivatives indicated that a 2-benzyloxy derivative showed potent antagonism (Table 3).¹⁸ Substituted 2-benzylthio derivatives (**32–36**) exhibited similar and reasonable antagonism with a range of $K_{i(\text{CAP})} = 2.3\text{--}8.7$ nM but were less potent than the corresponding 2-benzyloxy surrogates. 2-Arylmethylthio derivatives (**37, 38**) showed further reduced activities. The 2-phenylethylthio derivative (**39**) displayed good antagonism.

Detailed in vitro activity of **24S**, the most promising antagonist in this study, was investigated for multiple TRPV1 activators including capsaicin, *N*-arachidonoyl dopamine (NADA), pH and heat (45 °C), and compared to the activity of lead **2** (Table 4). Compound **24S** showed excellent antagonism of capsaicin and NADA comparable to **2**, but showed poor antagonism toward pH and heat, in contrast to **2**. The differential activity of **24S** compared to **2** is consistent with the different in vivo responses described below.

2.3. In vivo activity

The analgesic activity of compound **24S** was evaluated orally in the rat Bennett model²⁰ as a neuropathic pain model and its activity was compared to those of reference compounds **1**, **2** and pregabalin (Fig. 3). Previously, we reported that antagonist **2** showed excellent anti-allodynic efficacy in that model with ED₅₀ = 0.9 mg/Kg po (max 60% at 3.16 mg/Kg) and was better than **1** (ED₅₀ = 26.6 mg/Kg, max 59% at 46.4 mg/Kg) and pregabalin (ED₅₀ = 42.2 mg/Kg, max 69% at 100 mg/Kg).¹⁷ We now find that the analgesic potency of **24S** showed dose-dependent efficacy with ED₅₀ = 0.19 mg/Kg po (max 75% at 10 mg/Kg) and was superior to **2**.

Consistent with its in vitro mechanism of action, in vivo **24S** also blocked response to capsaicin (Fig. 4). The intraperitoneal injection of 3 mg/Kg capsaicin resulted in a decrease of body temperature as expected,^{21,22} with a reduction from 37.6 ± 0.1 to 34.0 ± 0.1 °C (*p* < 0.05) at 15 min post capsaicin injection and to 35.8 ± 0.4 °C (*p* < 0.05) at 30 min post capsaicin injection. By 60 min body temperature had returned to normal (37.1 ± 0.1 to 37.0 ± 0.1 °C; *p* = 1.00). The oral administration of 0.3 mg/Kg **24S** (15 min before capsaicin injection) completely inhibited the effect of capsaicin on body temperature at 30 min, with partial inhibition of the effect at 15 min.

2.4. Molecular modeling

In order to investigate the binding interactions of **24S**, a flexible docking study was performed using our human TRPV1 (hTRPV1) model¹⁷ built based on our rat TRPV1 (rTRPV1) model.²³ The docking result demonstrated that **24S** binds very well at the capsaicin binding site, as we had previously described for **2**.¹⁷ The 4-(methylsulfonylamino)phenyl group (A-region) occupied the deep bottom hole and was involved in hydrophobic interactions with Tyr511 and Ile564 (Fig. 5). The fluorine atom of the A-region participated in hydrogen bonding with Lys571. The amide group (B-region) made a hydrogen bond with Tyr511 and also contributed to the appropriate positioning of the C-region for hydrophobic interactions.

In the C-region, the cyclohexylthio group initially was expected to orient toward the hydrophobic region composed of Met514 and Leu515 as did the 4-methylpiperidinyl group of **2**.¹⁷ However, the modeling indicated that the cyclohexyl ring was extended toward the upper hydrophobic pocket composed of Leu547 and Thr550 to generate the hydrophobic interaction, and the sulfur atom made the hydrophobic interaction with Leu515. It seems that the bent conformation of the thioether linker allowed the cyclohexylthio group to make hydrophobic interactions with both hydrophobic regions. In addition, the pyridine ring nitrogen in the C-region made a hydrogen bond with Tyr511.

3. Conclusion

The structure activity relationships of 2-thio pyridine C-region derivatives of 2-(3-fluoro-4-methylsulfonylaminophenyl)propanamides as *h*TRPV1 antagonists were investigated. The analysis indicated that 2-cycloalkylthio derivatives showed better antagonism than the corresponding 2-alkylthio ones, in contrast to the findings for a series of 2-alkyloxy derivatives. Among the 2-thio pyridine derivatives, compound **24S** showed stereospecific and excellent TRPV1 antagonism with $K_{i(\text{CAP})} = 0.4$ nM. It demonstrated dose-dependent and strong anti-allodynic activity with $\text{ED}_{50} = 0.19$ - mg/Kg po (max 75% at 10 mg/Kg) in a neuropathic pain model in the rat and was superior to previous lead **2**. Consistent with its action in vitro being through TRPV1, compound **24S** blocked capsaicin-induced hypothermia. Docking analysis of **24S** with our *h*TRPV1 homology model indicated that the 2-(3-fluoro-4-methylsulfonylaminophenyl)propanamide (A and B-regions) made critical hydrophobic and hydrogen bonding interactions with Tyr511, and the cyclohexyl group and the sulfur atom in the C-region made two hydrophobic interactions with the pocket composed of Leu547/Thr550 and Leu515, respectively.

4. Experimental

4.1. Chemistry

4.1.1. General—All chemical reagents were commercially available. Melting points were determined on a Büchi Melting Point B-540 apparatus and are uncorrected. Silica gel column chromatography was performed on silica gel 60,230–400 mesh, Merck. Nuclear magnetic resonance spectra were recorded on a JEOL JNM-LA 300 and Bruker Avance 400 MHz FT-NMR spectrometer. Chemical shifts are reported in ppm units with Me_4Si as a reference standard. Mass spectra were recorded on a VG Trio-2 GC-MS and 6460 Triple Quad LC/MS. All final compounds were purified to >95% purity, as determined by high-performance liquid chromatography (HPLC). HPLC was performed on an Agilent 1120 Compact LC (G4288A) instrument using a Agilent Eclipse Plus C18 column (4.6 × 250 mm, 5 μm) and Daicel Chiralcel OD-H column (4.6 × 250 mm, 5 μm). Optical rotations were measured in a JASCO DIP-2000 digital polarimeter.

4.1.2. General procedure for the synthesis of **4**

4.1.2.1. Method A: A mixture of compound **3** (2 mmol), thiol (4 mmol) and DBU (4 mmol) were dissolved in acetonitrile (15 mL) and stirred for 12 h at room temperature. The reaction mixture was diluted with water and extracted with EtOAc several times. The combined organic extracts were dried over MgSO_4 , filtered, and concentrated in vacuo. The residue was purified by flash column chromatography on silica gel using EtOAc:hexanes = 1:15 as eluant.

4.1.2.2. Method B: A solution of thiol (2.4 mmol) in DMF (5 mL) was treated with sodium hydride (2.6 mmol). The resulting suspension was cooled to 0 °C and compound **3** (2 mmol) was added. After stirring overnight at room temperature, the reaction mixture was diluted with water and extracted with EtOAc several times. The combined organic extracts

were dried over MgSO₄, filtered, and concentrated in vacuo. The residue was purified by flash column chromatography on silica gel using EtOAc:hexanes = 1:15 as eluant.

4.1.3. General procedure for the synthesis of 5—To a stirred solution of nitrile (2 mmol) in anhydrous THF (10 mL) was added BH₃–SMe₂ (2.0 M in THF, 3 mL, 6 mmol) at room temperature. After being refluxed for 8 h, the mixture was cooled to room temperature, 2 N HCl was added, and the solution then refluxed for 30 min. After cooling to room temperature, the mixture was neutralized with 2 N NaOH and extracted with EtOAc several times. The combined organic layers were washed with brine, dried over MgSO₄, and concentrated in vacuo. The residue was purified by flash column chromatography on silica gel using CH₂Cl₂:MeOH = 10:1 as eluant.

4.1.4. General procedure for the syntheses of 7–39—A mixture of amine **5** (1.2 mmol), acid **6** (1.0 mmol) and 1-(3-dimethylaminopropyl)-3-ethyl-carbodiimide hydrochloride (1.2 mmol) in DMF (5 mL) was stirred for 12 h at room temperature. The reaction mixture was diluted with water and extracted with EtOAc several times. The aqueous phase was saturated with NaCl and extracted with EtOAc again. The combined organic extracts were washed with 1 N HCl and brine, dried over MgSO₄, filtered, and concentrated in vacuo. The residue was purified by flash column chromatography on silica gel using EtOAc:hexanes = 1:2 as eluant.

4.1.4.1. 2-(3-Fluoro-4-methanesulfonylamino-phenyl)-N-(2-(butylthio)-6-(trifluoromethyl)pyridin-3-ylmethyl)propionamide (7): 71% Yield, white solid, mp = 105–107 °C, ¹H NMR (300 MHz, CDCl₃) δ 7.50–7.42 (m, 2H), 7.27 (s, 1H), 7.13 (dd, 1H, *J* = 8.1 Hz), 7.07 (d, 1H, *J* = 8.1 Hz), 6.98 (br s, 1H), 6.33 (br t, 1H), 4.36 (m, 2H), 3.56 (q, 1H, *J* = 6.9 Hz), 3.22 (t, 2H, *J* = 7.5 Hz), 3.01 (s, 3H), 1.66 (m, 2H), 1.50–1.38 (m, 5H), 0.93 (t, 3 H, *J* = 7.2 Hz); MS (FAB) *m/z* 508 (M+H).

4.1.4.2. 2-(3-Fluoro-4-(methylsulfonamido)phenyl)-N-(2-(pentylthio)-6-(trifluoromethyl)pyridin-3-ylmethyl)propanamide (8): 65% Yield, white solid, mp = 126–129 °C, ¹H NMR (300 MHz, CDCl₃) δ 7.52–7.42 (m, 2H), 7.27 (s, 1H), 7.13 (dd, 1H, *J* = 8.0 Hz), 7.07 (d, 1H, *J* = 8.2 Hz), 6.98 (br s, 1H), 6.33 (br t, 1H), 4.36 (m, 2H), 3.58 (q, 1 H, *J* = 6.9 Hz), 3.25 (t, 2 H, *J* = 7.5 Hz), 3.05 (s, 3H), 1.66 (m, 2H), 1.58–1.48 (m, 5H), 1.23–1.09 (m, 2H), 0.90 (t, 3 H, *J* = 7.1 Hz); MS (FAB) *m/z* 522 (M+H).

4.1.4.3. 2-(3-Fluoro-4-(methylsulfonamido)phenyl)-N-(2-(hexylthio)-6-(trifluoromethyl)pyridin-3-ylmethyl)propanamide (9): 72% Yield, white solid, mp = 102–105 °C, ¹H NMR (300 MHz, CDCl₃) δ 7.51–7.40 (m, 2H), 7.24 (s, 1H), 7.11 (dd, 1H, *J* = 8.1 Hz), 7.05 (d, 1H, *J* = 8.0 Hz), 6.94 (br s, 1H), 6.31 (br t, 1H), 4.31 (m, 2H), 3.58 (q, 1H, *J* = 6.7 Hz), 3.24 (t, 2H, *J* = 7.3 Hz), 3.03 (s, 3H), 1.66 (m, 2H), 1.58–1.48 (m, 5H), 1.24–1.02 (m, 4H), 0.91 (t, 3 H, *J* = 7.2 Hz); MS (FAB) *m/z* 536 (M+H).

4.1.4.4. 2-(3-Fluoro-4-(methylsulfonamido)phenyl)-N-(2-(isopentylthio)-6-(trifluoromethyl)pyridin-3-ylmethyl)propanamide (10): 81% Yield, white solid, mp = 123–126 °C, ¹H NMR (300 MHz, CDCl₃) δ 7.50–7.41 (m, 2H), 7.28 (s, 1H), 7.12 (dd, 1 H, *J* = 8.1 Hz), 7.07 (d, 1H, *J* = 8.1 Hz), 6.98 (br s, 1H), 6.33 (br t, 1H), 4.36 (m, 2H), 3.56 (q, 1

H, $J = 6.9$ Hz), 3.22 (t, 2 H, $J = 7.5$ Hz), 3.01 (s, 3H), 1.93–1.83 (m, 1H), 1.66 (m, 2H), 1.18 (d, 3H, $J = 7.2$ Hz), 0.96 (d, 6 H, $J = 7.1$ Hz); MS (FAB) m/z 522 (M+H).

4.1.4.5. 2-(3-Fluoro-4-(methylsulfonamido)phenyl)-N-((2-(2,2,2-trifluoroethylthio)-6-(trifluoromethyl)pyridin-3-yl)methyl) propanamide (11): 75% Yield, white solid, mp = 164–166 °C, ^1H NMR (300 MHz, CDCl_3) δ 7.55–7.42 (m, 2H), 7.32 (s, 1H), 7.16 (dd, 1H, $J = 8.0$ Hz), 7.07 (d, 1 H, $J = 8.1$ Hz), 6.96 (br s, 1H), 6.32 (br t, 1H), 4.36 (m, 2H), 3.59 (q, 1 H, $J = 6.9$ Hz), 3.45 (s, 2H), 3.00 (s, 3H); MS (FAB) m/z 534 (M+H).

4.1.4.6. N-((2-(3-Bromopropylthio)-6-(trifluoromethyl)pyridin-3-yl)methyl)-2-(3-fluoro-4-(methylsulfonamido)phenyl)propanamide (12): 40% Yield, white solid, mp = 100–103 °C, ^1H NMR (300 MHz, CDCl_3) δ 7.48–7.56 (m, 2H), 7.32 (d, 1H, $J = 7.8$ Hz), 7.15–7.07 (m, 2H), 6.62 (bs, 1H), 6.03 (br t, 1H), 4.38 (d, 2H, $J = 5.7$ Hz), 3.60–3.49 (m, 3H), 3.37 (t, 2H, $J = 6.9$ Hz), 3.03 (s, 3H), 2.26 (m, 2H), 1.50 (d, 3 H, $J = 6.9$ Hz); MS (FAB) m/z 573 (M+H).

4.1.4.7. 2-(3-Fluoro-4-(methylsulfonamido)phenyl)-N-((2-(3-hydroxypropylthio)-6-(trifluoromethyl)pyridin-3-yl)methyl) propanamide (13): 65% Yield, white solid, mp = 93–95 °C, ^1H NMR (300 MHz, CDCl_3) δ 7.57 (dd, 1H, $J = 7.8$ and 7.8 Hz), 7.49 (d, 1H, $J = 7.8$ Hz), 7.33 (d, 1H, $J = 7.8$ Hz), 7.06–7.12 (m, 2H), 6.61 (bs, 1H), 5.97 (br t, 1H), 4.39 (d, 2H, $J = 5.7$ Hz), 3.70 (m, 2h), 3.54 (q, 1H, $J = 6.9$ Hz), 3.36 (m, 2H), 3.03 (s, 3H), 1.96 (m, 2H), 1.50 (d, 3 H, $J = 6.9$ Hz); MS (FAB) m/z 510 (M+H).

4.1.4.8. N-((2-(3-(Dimethylamino)propylthio)-6-(trifluoromethyl)pyridin-3-yl)methyl)-2-(3-fluoro-4-(methylsulfonamido)phenyl)propanamide (14): 33% Yield, white solid, mp = 130–133 °C, ^1H NMR (300 MHz, CDCl_3) δ 7.58–7.49 (m, 2H), 7.33 (d, 1H, $J = 6$ Hz), 7.15–7.08 (m, 2H), 5.99 (m, 1H), 4.40–4.37 (m, 2H), 3.56 (q, 1H, $J = 6$ Hz), 3.21–3.17 (m, 2H), 3.03 (s, 3H), 2.90–2.84 (m, 2H), 2.57 (s, 6H), 2.22–2.14 (m, 2H), 1.50 (d, 3H, $J = 6.0$ Hz); MS (FAB) m/z 537 (M+H).

4.1.4.9. 2-(3-Fluoro-4-(methylsulfonamido)phenyl)-N-((2-(3-(pyrrolidin-1-yl)propylthio)-6-(trifluoromethyl)pyridin-3-yl) methyl)propanamide (15): 78% Yield, white solid, mp = 139–141 °C, ^1H NMR (300 MHz, CDCl_3) δ 7.49–7.35 (m, 3H), 7.23–7.12 (m, 2H), 4.39–4.25 (m, 2H), 3.74 (q, 1 H, $J = 6.0$ Hz), 3.30 (m, 1H), 3.21 (t, 1H, $J = 6.0$ Hz), 3.10–3.03 (m, 1H), 2.98 (s, 3H), 2.89–2.84 (m, 1H), 2.80 (s, 3H), 2.25–2.14 (m, 1H), 2.09–2.00 (m, 1H), 1.94–1.85 (m, 1H), 1.46 (d, 3 H, $J = 6.0$ Hz); MS (FAB) m/z 563 (M+H).

4.1.4.10. 2-(3-Fluoro-4-(methylsulfonamido)phenyl)-N-((2-(3-(piperidin-1-yl)propylthio)-6-(trifluoromethyl)pyridin-3-yl)methyl)propanamide (16): 76% Yield, white solid, mp = 137–139 °C, ^1H NMR (300 MHz, CDCl_3) δ 7.57 (d, 1 H, $J = 7.7$ Hz), 7.45 (t, 1H, $J = 8.0$ Hz), 7.28–7.26 (m, 2H), 7.07 (d, 1H, $J = 9.18$ Hz), 6.87 (br s, 1H), 4.43–4.25 (m, 2H), 3.69 (q, 1H), 3.15 (t, 2H, $J = 7.14$ Hz), 2.99 (s, 3H), 2.83–2.77 (m, 4H), 2.05–1.95 (m, 2H), 1.85 (t, 3 H, $J = 5.31$ Hz), 1.57 (br s, 1H), 1.48 (d, 2 H, $J = 7.14$ Hz), 1.26 (s, 3H), 0.87 (m, 1H); MS (FAB) m/z 577 (M+H).

4.1.4.11. 2-(3-Fluoro-4-(methylsulfonamido)phenyl)-N-((2-(3-(4-methylpiperidin-1-yl)propylthio)-6-(trifluoromethyl)pyridin-3-yl)methyl)propanamide (17): 82% Yield, white solid, mp = 75–78 °C, ¹H NMR (300 MHz, CDCl₃) δ 7.64–7.45 (m, 2H), 7.32 (d, 1H, *J* = 9.0 Hz), 7.16–7.09 (m, 2H), 4.44–4.34 (m, 2H), 3.56 (q, 1 H, *J* = 9.0 Hz), 3.25–3.17 (m, 2H), 3.05–2.84 (m, 9H), 2.17–2.07 (m, 2H), 0.97 (d, 3 H, *J* = 6.0 Hz); MS (FAB) *m/z* 591 (M+H).

4.1.4.12. 2-(3-Fluoro-4-(methylsulfonamido)phenyl)-N-((2-(3-morpholinopropylthio)-6-(trifluoromethyl)pyridin-3-yl)methyl) propanamide (18): 81% Yield, white solid, mp = 80–85 °C, ¹H NMR (300 MHz, CDCl₃) δ 7.59–7.48 (m, 2H), 7.30 (d, 1H, *J* = 7.68 Hz), 7.07–7.00 (m, 2H), 5.97 (t, 1H), 4.44–4.28 (m, 2H), 3.75 (t, 6H, *J* = 4.38 Hz), 3.55 (q, 1H), 3.27–3.13 (m, 2H), 3.01 (s, 3H), 2.47–2.42 (m, 6H), 1.82–1.74 (m, 2H), 1.51–1.48 (d, 4 H, *J* = 6.96 Hz); MS (FAB) *m/z* 579 (M+H).

4.1.4.13. 2-(3-Fluoro-4-(methylsulfonamido)phenyl)-N-((2-(2-phenoxyethylthio)-6-(trifluoromethyl)pyridin-3-yl)methyl)propanamide (19): 69% Yield, white solid, mp = 88–90 °C, ¹H NMR (300 MHz, CDCl₃) δ 7.58–7.45 (m, 2H), 7.38–7.26 (m, 4H), 7.14–7.04 (m, 2H), 6.98–6.92 (m, 3H), 6.10–6.08 (m, 1H), 4.46–4.30 (m, 1H), 4.26 (t, 2H, *J* = 6.39 Hz), 3.63 (t, 2H, *J* = 6.39 Hz), 3.53 (q, 1 H, *J* = 6.0 Hz), 3.00 (s, 3H), 1.48 (d, 3 H, *J* = 6.0 Hz); MS (FAB) *m/z* 572 (M+H).

4.1.4.14. 3-(3-((2-(3-Fluoro-4-(methylsulfonamido)phenyl) propanamido)methyl)-6-(trifluoromethyl)pyridin-2-ylthio) propanoic acid (20): 60% Yield, yellow solid, mp = 135–137 °C, ¹H NMR (300 MHz, CDCl₃) δ 11.9 (s, 1H), 7.56–7.55 (m, 3H), 7.30 (d, 1H, *J* = 7.8 Hz), 7.34 (s, 1H), 7.13–7.09 (m, 2H), 6.72 (bs, 1H), 6.11 (br t, 1H), 4.32 (m, 2H), 3.53 (q, 1H, *J* = 6.9 Hz), 3.46 (t, 2H, *J* = 6.6 Hz), 3.02 (s, 3H), 2.81 (t, 2H, *J* = 6.7 Hz), 1.53 (d, 3 H, *J* = 6.9 Hz); MS (FAB) *m/z* 524 (M+H).

4.1.4.15. Methyl 3-(3-((2-(3-fluoro-4-(methylsulfonamido)phenyl) propanamido)methyl)-6-(trifluoromethyl)pyridin-2-ylthio) propanoate (21): 68% Yield, white solid, mp = 117–120 °C, ¹H NMR (300 MHz, CDCl₃) δ 7.57–7.46 (m, 3H), 7.31 (d, 1H, *J* = 7.8 Hz), 7.34 (s, 1H), 7.14–7.01 (m, 2H), 6.74 (bs, 1H), 6.15 (br t, 1H), 4.35 (m, 2H), 3.70 (s, 3H), 3.55 (q, 1H, *J* = 6.9 Hz), 3.47 (t, 2H, *J* = 6.6 Hz), 3.02 (s, 3H), 2.78 (t, 2H, *J* = 6.6 Hz), 1.50 (d, 3H, *J* = 6.9 Hz); MS (FAB) *m/z* 538 (M+H).

4.1.4.16. 2-(3-Fluoro-4-(methylsulfonamido)phenyl)-N-((2-(3-oxo-3-(pyrrolidin-1-yl)propylthio)-6-(trifluoromethyl)pyridin-3-yl)methyl)propanamide (22): 42% Yield, pale yellow solid, mp = 94–96 °C, ¹H NMR (300 MHz, CDCl₃) δ 7.56–7.55 (m, 3H), 7.30 (d, 1H, *J* = 7.8 Hz), 7.34 (s, 1H), 7.13–7.09 (m, 2H), 6.72 (bs, 1H), 6.11 (br t, 1H), 4.32 (m, 2H), 3.53 (q, 1 H, *J* = 6.9 Hz), 3.49 (t, 4H, *J* = 7.9 Hz), 3.36 (t, 2H, *J* = 6.7 Hz), 3.04 (s, 3H), 2.80 (t, 2H, *J* = 6.7 Hz), 1.87–1.82 (m, 4H), 1.54 (d, 3H, *J* = 6.9 Hz); MS (FAB) *m/z* 573 (M+H).

4.1.4.17. N-((2-(Cyclopentylthio)-6-(trifluoromethyl)pyridin-3-yl)methyl)-2-(3-fluoro-4-(methylsulfonamido)phenyl)propanamide (23): 59% Yield, yellow solid, mp = 126–129 °C, ¹H NMR (300 MHz, CDCl₃) δ 7.50 (t, 2 H, *J* = 9.0 Hz), 7.27 (d, 1H, *J* = 9.0

Hz), 7.14–7.06 (m, 2H), 6.59 (s, 1H), 6.03 (m, 1H), 4.42–4.29 (m, 2H), 4.16–4.07 (m, 1H), 3.55 (q, 1H, $J = 9.0$ Hz), 3.02 (s, 2H), 2.27–2.17 (m, 4H), 1.75–1.48 (m, 7H); MS (FAB) m/z 520 (M+H).

4.1.4.18. *N*-((2-(Cyclohexylthio)-6-(trifluoromethyl)pyridin-3-yl)methyl)-2-(3-fluoro-4-(methylsulfonamido)phenyl)propanamide (**24**): 65% Yield, white solid, mp = 70–73 °C, ^1H NMR (300 MHz, CD_3OD) δ 7.48–7.35 (m, 3H), 7.26 (d, 1H, $J = 7.8$ Hz), 7.16 (dd, 1H, $J = 1.8$ and 11.1 Hz), 7.10 (d, 1H, $J = 8.4$ Hz), 6.13 (br s, 1H), 4.35 (d, 2H, $J = 5.7$ Hz), 3.82 (m, 1H), 3.56 (q, 1H, $J = 7.2$ Hz), 3.02 (s, 3H), 2.06 (m, 2H), 1.75 (m, 2H), 1.49 (d, 3H, $J = 7.2$ Hz), 1.33–1.26 (m, 6H); MS (FAB) m/z 534 (M+H).

4.1.4.19. (*S*)-*N*-((2-(Cyclohexylthio)-6-(trifluoromethyl)pyridin-3-yl)methyl)-2-(3-fluoro-4-(methylsulfonamido)phenyl)propanamide (**24S**): $[\alpha]_{\text{D}}^{25} + 18.2$ (c 0.1, MeOH), 99% ee, The spectra are identical to those of compound **24**.

4.1.4.20. (*R*)-*N*-((2-(Cyclohexylthio)-6-(trifluoromethyl)pyridin-3-yl)methyl)-2-(3-fluoro-4-(methylsulfonamido)phenyl)propanamide (**24R**): $[\alpha]_{\text{D}}^{25} - 18.5$ (c 0.1, MeOH), 98.5% ee, The spectra are identical to those of compound **24**.

4.1.4.21. *N*-((2-(Cyclohexylsulfinyl)-6-(trifluoromethyl)pyridin-3-yl)methyl)-2-(3-fluoro-4-(methylsulfonamido)phenyl)propanamide (**25**): 78% Yield, white solid, mp = 68–70 °C, ^1H NMR (300 MHz, DMSO) δ 9.51 (s, 1H), 8.61 (d, 1H), 8.05 (d, 1H), 8.00 (m, 1H), 7.31 (m, 1H), 7.22 (m, 1H), 7.15 (m, 1H), 4.74 (d, 2H), 3.78 (m, 2H), 3.02 (s, 3H), 1.93 (br s, 2H), 1.81 (d, 2H), 1.65 (m, 2H), 1.47 (m, 2H), 1.31–1.21 (m, 5 H); MS (FAB) m/z 520 (M+H).

4.1.4.22. *N*-((2-(Cyclohexylsulfonyl)-6-(trifluoromethyl)pyridin-3-yl)methyl)-2-(3-fluoro-4-(methylsulfonamido)phenyl)propanamide (**26**): 67% Yield, white solid, mp = 68–71 °C, ^1H NMR (300 MHz, DMSO) δ 9.52 (s, 1H), 8.63 (d, 1H), 8.15 (d, 1H), 8.00 (m, 1H), 7.34 (m, 1H), 7.24 (m, 1H), 7.15 (m, 1H), 4.63 (d, 2H), 3.71 (m, 2H), 3.01 (s, 3H), 1.81–1.69 (m, 4H), 1.59–1.50 (m, 4H), 1.37 (d, 3H), 1.25–1.15 (m, 4 H); MS (FAB) m/z 566 (M+H)

4.1.4.23. 2-(3-Fluoro-4-(methylsulfonamido)phenyl)-*N*-((2-(4-methylcyclohexylthio)-6-(trifluoromethyl)pyridin-3-yl)methyl)propanamide (**27**): 66% Yield, white solid, mp = 70–75 °C, ^1H NMR (300 MHz, DMSO) δ 9.52 (s, 1H), 8.59 (d, 1H), 7.51 (d, 1H), 7.35 (m, 1H), 7.25 (m, 1H), 7.15 (m, 1H), 4.25 (d, 2H), 4.00 (m, 2H), 3.75 (m, 2H), 3.01 (s, 3H), 1.85 (s, 2H), 1.60–1.48 (m, 4H), 1.28–1.18 (m, 3H), 0.91 (d, 3 H); MS (FAB) m/z 548 (M+H).

4.1.4.24. 2-(3-Fluoro-4-(methylsulfonamido)phenyl)-*N*-((2-(2-methylcyclohexylthio)-6-(trifluoromethyl)pyridin-3-yl)methyl)propanamide (**28**): 65% Yield, white solid, mp = 75–78 °C, ^1H NMR (300 MHz, DMSO) δ 9.52 (s, 1H), 8.59 (d, 1H), 7.51 (d, 1H), 7.35 (m, 1H), 7.25 (m, 1H), 7.15 (m, 1H), 4.31 (d, 2H), 4.25 (m, 2H), 3.75 (m, 2H), 3.01 (s, 3H), 1.80 (s, 2H), 1.60–1.48 (m, 4H), 1.40–1.37 (m, 3H), 0.91 (d, 3 H); MS (FAB) m/z 548 (M+H).

4.1.4.25. *N*-((2-(4-Ethylcyclohexylthio)-6-(trifluoromethyl)pyridin-3-yl)methyl)-2-(3-fluoro-4-(methylsulfonamido)phenyl)propanamide (**29**): 77% Yield, white solid, mp = 73–76 °C, ¹H NMR (300 MHz, DMSO) δ 9.52 (s, 1H), 8.52 (t, 1H), 7.51 (d, 1H), 7.35 (t, 1H), 7.25 (d, 1H), 7.15 (d, 1H), 4.18 (d, 2H), 3.75 (m, 2H), 3.01 (s, 3H), 2.04 (m, 2H), 1.75 (m, 3H), 1.25–1.00 (m, 4H), 0.91 (d, 5 H); MS (FAB) *m/z* 562 (M+H).

4.1.4.26. *N*-((2-(4-*tert*-Butylcyclohexylthio)-6-(trifluoromethyl)pyridin-3-yl)methyl)-2-(3-fluoro-4-(methylsulfonamido)phenyl)propanamide (**30**): 74% Yield, white solid, mp = 86–90 °C, ¹H NMR (300 MHz, DMSO) δ 9.52 (s, 1H), 8.52 (t, 1H), 7.51 (d, 1H), 7.35 (t, 1H), 7.25 (d, 1H), 7.15 (d, 1H), 4.17 (d, 2H), 3.75 (m, 2H), 3.01 (s, 3H), 2.14 (m, 2H), 1.78 (m, 3H), 1.41 (s, 2H), 1.25–1.00 (m, 4H), 0.75 (d, 9 H); MS (FAB) *m/z* 590 (M+H).

4.1.4.27. *N*-((2-(Cyclohexylmethylthio)-6-(trifluoromethyl)pyridin-3-yl)methyl)-2-(3-fluoro-4-(methylsulfonamido)phenyl)propanamide (**31**): 75% Yield, white solid, mp = 130–132 °C, ¹H NMR (300 MHz, CDCl₃) δ 7.54–7.49 (m, 2H), 7.28 (d, 1 H, *J* = 7.8 Hz), 7.15–7.07 (m, 2H), 6.50 (bs, 1H), 6.00 (br t, 1H), 4.40 (m, 2H), 3.55 (q, 1 H, *J* = 6.9 Hz), 3.14 (d, 2 H, *J* = 6.6 Hz), 3.03 (s, 3H), 1.85 (m, 2H), 1.70–1.53 (m, 4H), 1.49 (d, 3H, *J* = 6.9 Hz), 0.95–1.28 (m, 5 H); MS (FAB) *m/z* 548 (M+H).

4.1.4.28. *N*-((2-(4-Chlorobenzylthio)-6-(trifluoromethyl)pyridin-3-yl)methyl)-2-(3-fluoro-4-(methylsulfonamido)phenyl)propanamide (**32**): 72% Yield, white solid, mp = 96–98 °C, ¹H NMR (300 MHz, CDCl₃) δ 7.55–7.48 (m, 2H), 7.36–7.31 (m, 3H), 7.24–7.23 (m, 1H), 7.13–7.04 (m, 2H), 6.47 (s, 1H), 5.88 (m, 1H), 4.42 (s, 2H), 4.34 (t, 2H, *J* = 6.0 Hz), 3.49 (q, 1H, *J* = 7.2 Hz), 3.02 (s, 3H), 1.47 (d, 3H, *J* = 7.2 Hz); MS (FAB) *m/z* 576 (M+H).

4.1.4.29. 2-(3-Fluoro-4-(methylsulfonamido)phenyl)-*N*-((2-(4-methylbenzylthio)-6-(trifluoromethyl)pyridin-3-yl)methyl)propanamide (**33**): 81% Yield, white solid, mp = 145–147 °C, ¹H NMR (300 MHz, CD₃OD) δ 7.47–7.36 (m, 3H), 7.28–7.26 (m, 2H), 7.22–7.12 (m, 2H), 7.04 (d, 2 H, *J* = 7.68 Hz), 4.41 (s, 2H), 4.28 (d, 2H, *J* = 5.31 Hz), 3.71 (q, 1H), 2.97 (s, 3H), 2.27 (s, 3H), 1.44 (d, 3H, *J* = 6.96 Hz); MS (FAB) *m/z* 556 (M+H).

4.1.4.30. 2-(3-Fluoro-4-(methylsulfonamido)phenyl)-*N*-((2-(4-methoxybenzylthio)-6-(trifluoromethyl)pyridin-3-yl)methyl)propanamide (**34**): 84% Yield, white solid, mp = 158–161 °C, ¹H NMR (300 MHz, CDCl₃) δ 7.55–7.45 (m, 2H), 7.34–7.30 (m, 3H), 7.17–7.03 (m, 2H), 6.84–6.80 (m, 2H), 6.60 (s, 1H), 5.97 (m, 1H), 4.42 (s, 2H), 4.38–4.27 (m, 2H), 3.78 (s, 3H), 3.50 (q, 1H, *J* = 6.0 Hz), 3.01 (s, 3H), 1.46 (d, 3H, *J* = 6.0 Hz); MS (FAB) *m/z* 572 (M+H).

4.1.4.31. *N*-((2-(2-Chlorobenzylthio)-6-(trifluoromethyl)pyridin-3-yl)methyl)-2-(3-fluoro-4-(methylsulfonamido)phenyl)propanamide (**35**): 85% Yield, white solid, mp = 161–163 °C, ¹H NMR (300 MHz, CDCl₃) δ 7.61–7.55 (m, 2H), 7.51–7.46 (m, 1H), 7.39–7.32 (m, 2H), 7.23–7.14 (m, 1H), 7.12–7.07 (m, 1H), 7.05–7.03 (m, 1H), 6.45 (s, 1H), 5.95 (m, 1H), 4.60 (s, 2H), 4.32 (m, 2H), 3.49 (q, 1H, *J* = 7.5 Hz), 3.02 (s, 3H), 1.45 (d, 3H, *J* = 7.5 Hz); MS (FAB) *m/z* 576 (M+H).

4.1.4.32. 2-(3-Fluoro-4-(methylsulfonamido)phenyl)-N-((6-(trifluoromethyl)-2-(3-(trifluoromethyl)benzylthio)pyridin-3-yl)methyl)propanamide (36): 70% Yield, white solid, mp = 165–167 °C, ¹H NMR (300 MHz, CDCl₃) δ 7.72 (s, 1H), 7.63–7.48 (m, 4H), 7.43–7.32 (m, 2H), 7.14–7.05 (m, 2H), 6.45 (s, 1H), 5.89 (m, 1H), 4.49 (s, 2H), 4.34 (m, 2H), 3.52 (q, 1 H, *J* = 6.0 Hz), 3.02 (s, 3H), 1.48 (d, 3 H, *J* = 9.0 Hz); MS (FAB) *m/z* 610 (M+H).

4.1.4.33. 2-(3-Fluoro-4-(methylsulfonamido)phenyl)-N-((2-(furan-2-ylmethylthio)-6-(trifluoromethyl)pyridin-3-yl)methyl)propanamide (37): 72% Yield, white solid, mp = 143–145 °C, ¹H NMR (300 MHz, CDCl₃) δ 7.59–7.48 (m, 2H), 7.35–7.33 (m, 2H), 7.13–7.04 (m, 2H), 6.49 (s, 1H), 6.29–6.28 (m, 2H), 5.95–5.93 (m, 1H), 4.53 (s, 2H), 4.35 (Septet, 2H), 3.52 (q, 1H), 3.03 (s, 2H), 1.58 (s, 2H), 1.48 (d, 3H), 1.25 (m, 4H), 0.95–0.8 (m, 3 H); MS (FAB) *m/z* 532 (m+H).

4.1.4.34. 2-(3-Fluoro-4-(methylsulfonamido)phenyl)-N-((2-(thiophen-2-ylmethylthio)-6-(trifluoromethyl)pyridin-3-yl)methyl)propanamide (38): 84% Yield, white solid, mp = 126–129 °C, ¹H NMR (300 MHz, CDCl₃) δ 7.57 (d, 1H, *J* = 6.0 Hz), 7.47 (t, 1H, *J* = 6.0 Hz), 7.34 (d, 1H, *J* = 6.0 Hz), 7.17–7.03 (m, 4H), 6.90–6.87 (m, 1H), 6.61 (s, 1H), 6.02 (t, 1 H, *J* = 6.0 Hz), 4.71 (s, 2H), 4.41–4.27 (septet, 2H), 3.51 (q, 1H, *J* = 6.0 Hz), 3.0 (s, 3H), 1.46 (d, 3H, *J* = 6.0 Hz); MS (FAB) *m/z* 548 (M+H).

4.1.4.35. 2-(3-Fluoro-4-(methylsulfonamido)phenyl)-N-((2-(phenethylthio)-6-(trifluoromethyl)pyridin-3-yl)methyl)propanamide (39): 68% Yield, white solid, mp = 135–139 °C, ¹H NMR (300 MHz, CD₃OD) δ 7.44 (d, 2H, *J* = 8.25 Hz), 7.35–7.15 (m, 10H), 4.33 (d, 2H, *J* = 3.12 Hz), 3.71 (q, 1H), 3.43 (t, 2H), 3.34 (t, 2H), 2.98 (s, 3H), 1.49 (d, 3 H, *J* = 7.14 Hz); MS (FAB) *m/z* 556 (M+H).

4.2. Molecular modeling

The 3D structure of the ligand was generated with Concord and energy minimized using mmFF94s force field and mmFF94 charge until the rms of Powell gradient was 0.05 kcal mol⁻¹ Å⁻¹ in SYB-YL-X 1.2 (Tripos Int., St. Louis, MO, USA). The flexible docking study on our hTRPV1 model^{17,23} was performed by GOLD v.5.0.1 (Cambridge Crystallographic Data Centre, Cambridge, UK), which uses a genetic algorithm (GA) and allows for full ligand flexibility and partial protein flexibility. The binding site was defined as 8 Å around the capsaicin docked in the hTRPV1 model. The side chains of the nine residues, which are important for ligand binding, (i.e., Tyr511, Ser512, Met514, Leu515, Leu518, Phe543, Leu547, Thr550, and Asn551) were set to be flexible with ‘crystal mode’ in GOLD. The ligand was docked using the GoldScore scoring function with 30 GA runs. Other parameters were set as default. All computation calculations were undertaken on Intel® Xeon™ Quad-core 2.5 GHz workstation with Linux Cent OS release 5.5.

4.3. Biological assay

The methods for in vitro and in vivo assays were reported in the previous literature.¹⁷

Acknowledgments

This research was supported by Research Grants from Grunenthal, Grants from the National Research Foundation of Korea (NRF) (R11-2007-107-02001-0), Grants from the National Leading Research Lab (NLRL) program (2011-0028885), and in part by the Intramural Research Program of NIH, Center for Cancer Research, NCI (Project Z1A BC 005270).

References and notes

1. Szallasi A; Blumberg PM *Pharmacol. Rev* 1999, 51, 159. [PubMed: 10353985]
2. Tominaga M; Caterina MJ; Malmberg AB; Rosen TA; Gilbert H; Skinner K; Raumann BE; Basbaum AI; Julius D *Neuron* 1998, 21, 531. [PubMed: 9768840]
3. Caterina MJ; Schumacher MA; Tominaga M; Rosen TA; Levine JD; Julius D *Nature* 1997, 389, 816. [PubMed: 9349813]
4. Zygmunt PM; Petersson J; Andersson DA; Chuang H-H; Sorgard M; Di Marzo V; Julius D; Hogestatt ED *Nature* 1999, 400, 452. [PubMed: 10440374]
5. Hwang SW; Cho H; Kwak J; Lee SY; Kang CJ; Jung J; Cho S; Min KH; Suh YG; Kim D; Oh U *Proc. Natl. Acad. Sci U.S.A* 2000, 97, 6155. [PubMed: 10823958]
6. Walpole CSJ; Wrigglesworth R *Capsaicin in the Study of Pain*; Academic Press: San Diego, CA, 1993; p 63.
7. Appendino G; Szallasi A *Life Sci.* 1997, 60, 681. [PubMed: 9064473]
8. Szallasi A; Cruz F; Geppetti P *Trends Mol. Med* 2006, 12, 545. [PubMed: 16996800]
9. Kym PR; Kort ME; Hutchins CW *Biochem. Pharmacol* 2009, 78, 211. [PubMed: 19481638]
10. Wong GY; Gavva NR *Brain Res. Rev* 2009, 60, 267. [PubMed: 19150372]
11. Gunthorpe MJ; Chizh BA *Drug Discovery Today* 2009, 14, 56. [PubMed: 19063991]
12. Lazar J; Gharat L; Khairathkar-Joshi N; Blumberg PM; Szallasi A *Exp. Opin. Drug Disc* 2009, 4, 159.
13. Voight EA; Kort ME *Exp. Opin. Ther. Pat* 2010, 20, 1.
14. Szolcsányi J; Sándor Z *Trend Pharmacol. Sci* 2012, 33, 646.
15. Szallasi A; Sheta M *Exp. Opin. Investig. Drug* 2012, 21, 1351.
16. Kim YS; Kil M-J; Kang S-U; Ryu H; Kim MS; Cho Y; Bhondwe RS; Thorat SA; Sun W; Liu K; Lee JH; Choi S; Pearce LV; Pavlyukovets VA; Morgan MA; Tran R; Lazar J; Blumberg PM; Lee J *Bioorg. Med. Chem* 2012, 20, 215. [PubMed: 22169633]
17. Kim MS; Ryu H; Kang DW; Cho S-H; Seo S; Park YS; Kim M-Y; Kwak EJ; Kim YS; Bhondwe RS; Kim HS; Park S.-g.; Son K; Choi S; DeAndrea-Lazarus I; Pearce LV; Blumberg PM; Frank R; Bahrenberg G; Stockhausen H; Kögel BY; Schiene K; Christoph T; Lee J *J. Med. Chem* 2012, 55, 8392. [PubMed: 22957803]
18. Thorat SA; Kang DW; Ryu H; Kim MS; Kim HS; Ann J; Ha T-H; Kim SE; Son K; Choi S; Blumberg PM; Frank R; Bahrenberg G; Schiene K; Christoph T; Lee J *Eur. J. Med. Chem* 2013, 64, 589. [PubMed: 23685943]
19. Ryu H; Jin M-K; Kang S-U; Kim SY; Kang DW; Lee J; Pearce LV; Pavlyukovets VA; Morgan MA; Tran R; Toth A; Lundberg DJ; Blumberg PM *J. Med. Chem* 2008, 51, 57. [PubMed: 18072720]
20. Bennett GJ; Xie Y-K *Pain* 1988, 33, 87. [PubMed: 2837713]
21. Szikszay M; Obál F Jr.; Obál F *Naunyn Schmiedeberg's Arch. Pharmacol* 1982, 320, 97. [PubMed: 7121619]
22. De Vries DJ; Blumberg PM *Life Sci.* 1989, 44, 711. [PubMed: 2927241]
23. Lee JH; Lee Y; Ryu H; Kang DW; Lee J; Lazar J; Pearce LV; Pavlyukovets VA; Blumberg PM; Choi SJ *Comput. Aided Mol. Des* 2011, 25, 317.

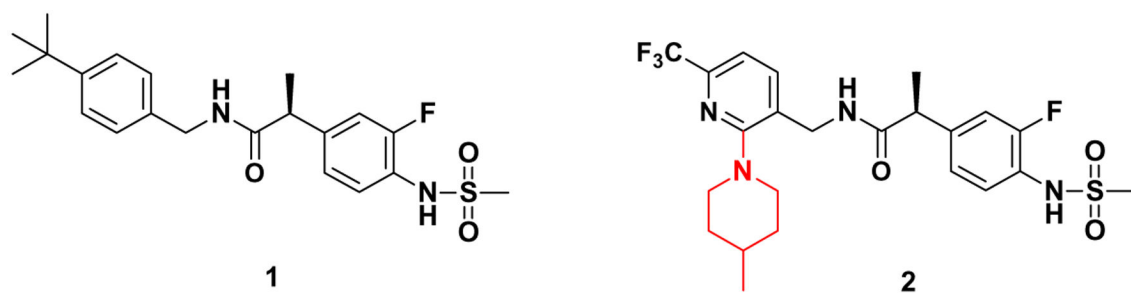


Figure 1.
Lead TRPV1 antagonists.

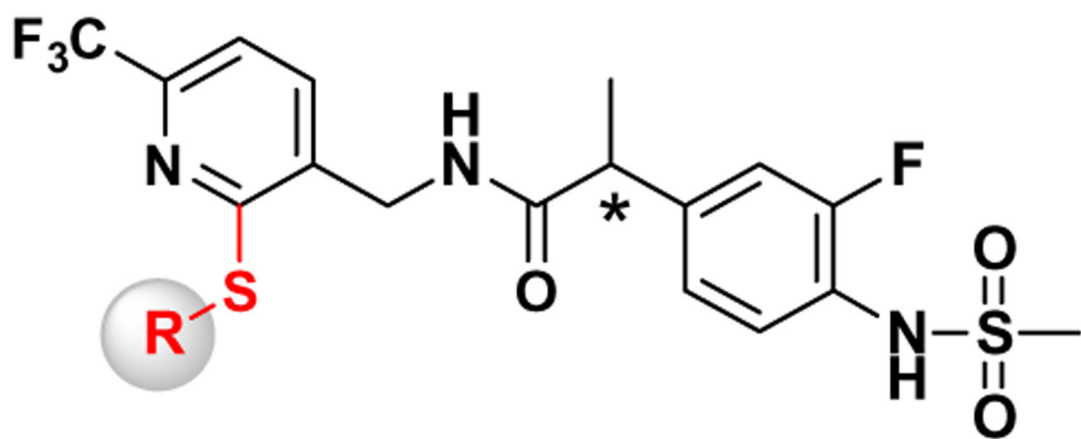


Figure 2.
General structure of the designed compounds.

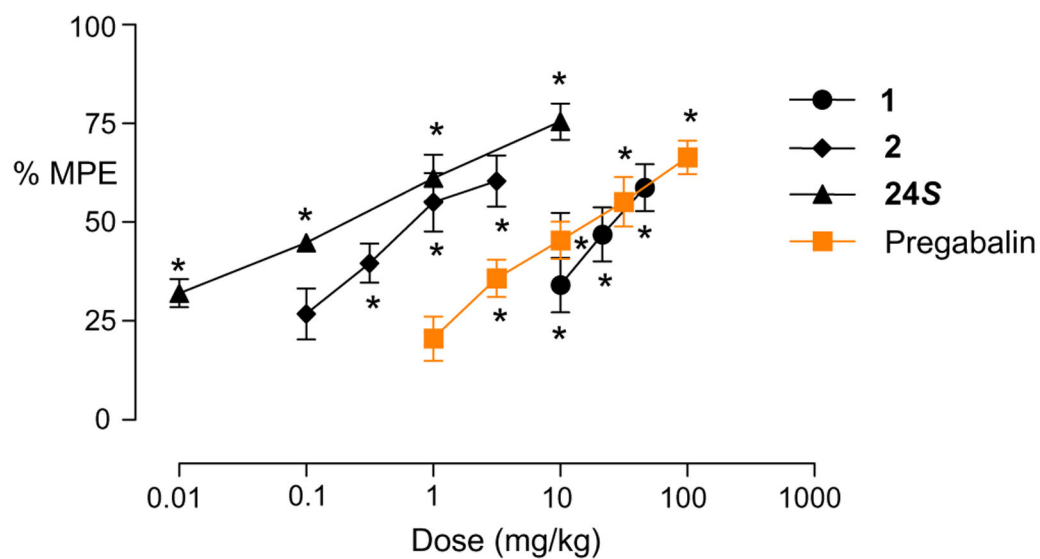


Figure 3. Comparison of analgesic activities of compound **24S** and reference compounds on CCI-induced cold allodynia after oral administration in rats. Data, $n = 10$, mean \pm SEM, $*p < 0.05$ versus vehicle. MPE, maximal possible effect.

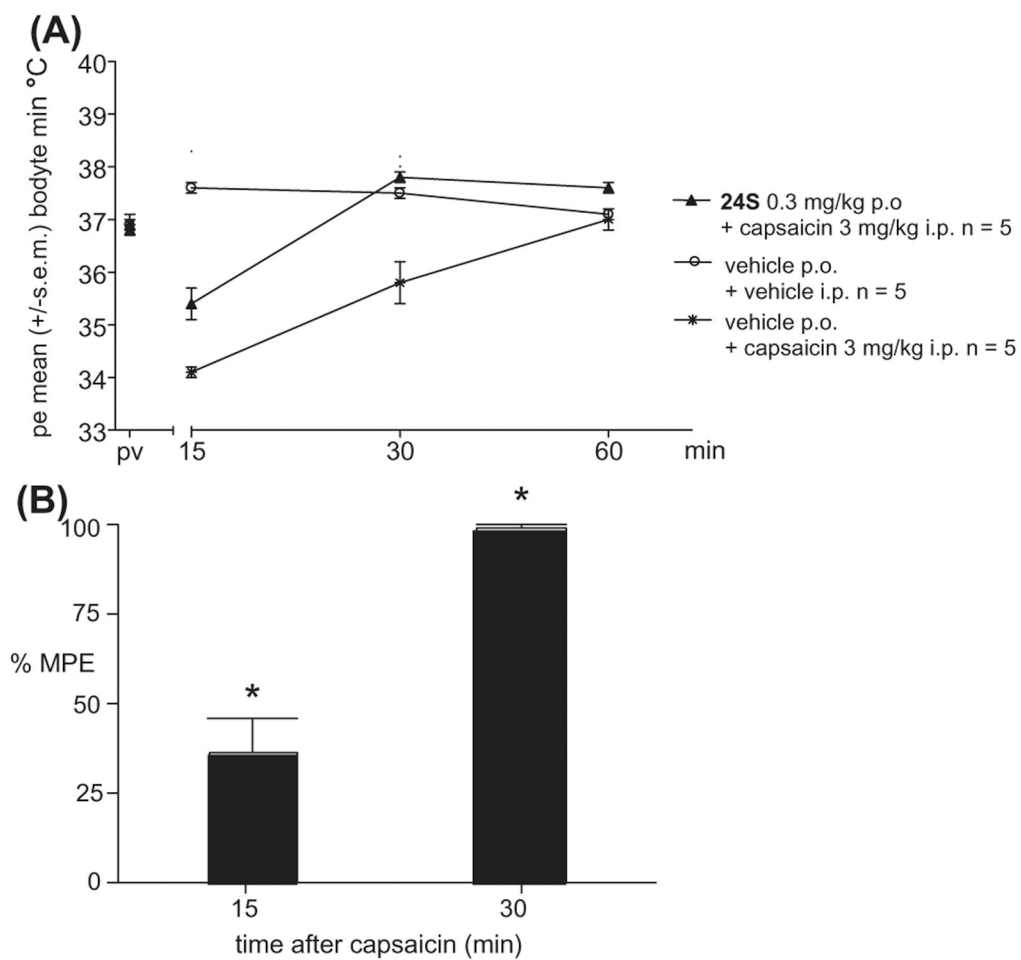


Figure 4. Effect of **24S** on capsaicin-induced hypothermia in mice. Data, $n = 5$, mean \pm SEM, * $p < 0.05$ versus vehicle. MPE, maximal possible effect of compound.

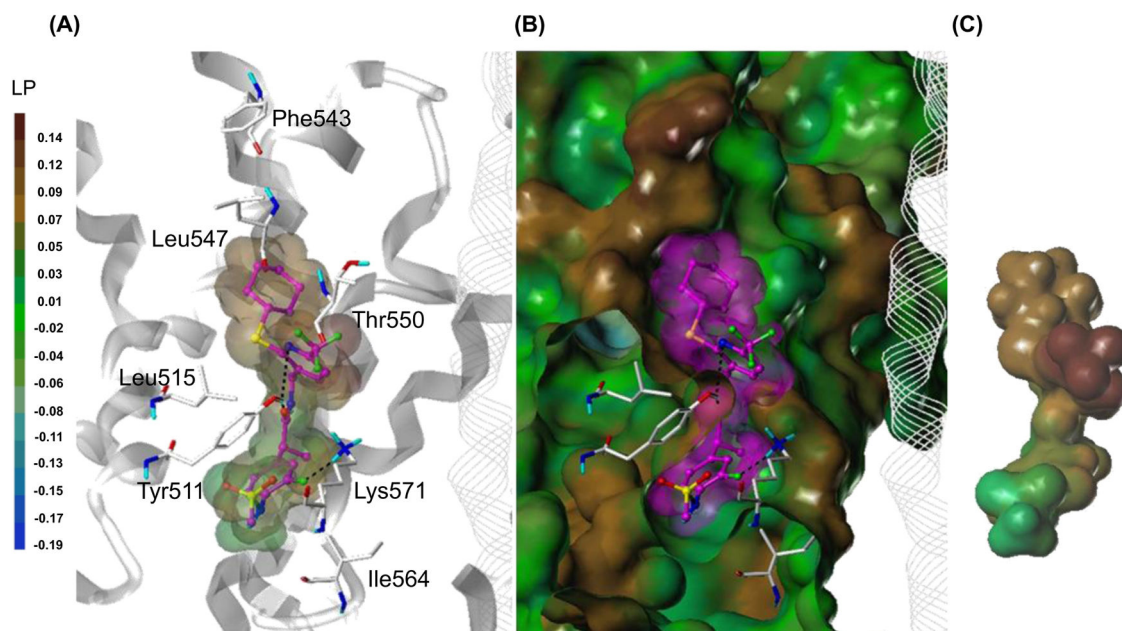
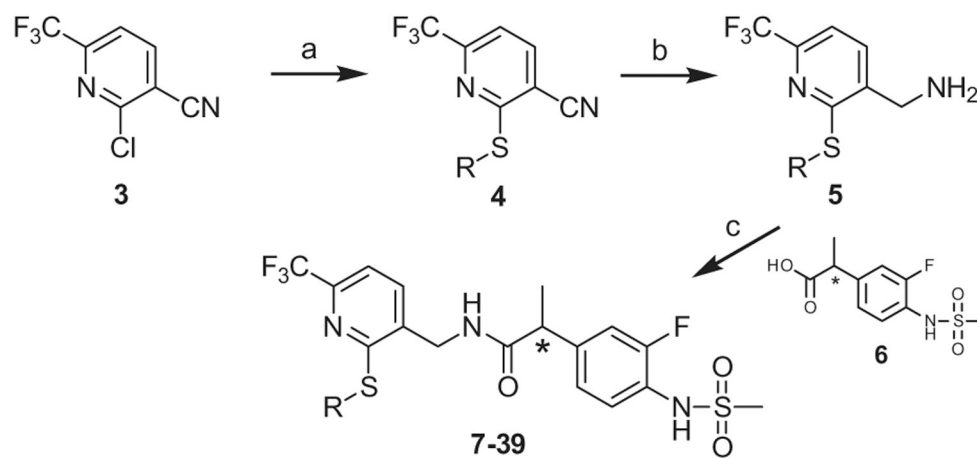


Figure 5.

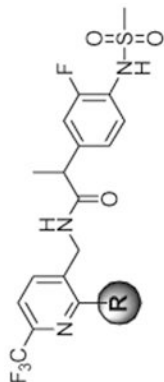
Flexible docking result of **24S** in the hTRPV1 model. (A) Binding mode of **24S**. The key interacting residues are marked and displayed as capped-stick with carbon atoms in white. The helices are colored in gray and the helices of the adjacent monomer are depicted in line ribbon. **24S** is displayed as ball-and-stick with carbon atoms in magenta. The van der Waals surface of the ligand is presented with its lipophilic potential property. Hydrogen bonds are shown as black dashed lines and non-polar hydrogens are undisplayed for clarity. (B) Surface representations of the docked ligand and hTRPV1. The Fast Connolly surface of hTRPV1 was generated by MOLCAD and colored by the lipophilic potential property. The surface of hTRPV1 is Z-clipped and that of the ligand is in its carbon color for clarity. (C) Van der Waals surface of the ligand colored by its lipophilic potential property.

**Scheme 1.**

Syntheses of 2-thio pyridine C-region analogues. Reagents and conditions: (a) [Method A] RSH, DBU, CH₃CN, rt; [Method B] RSH, NaH, DMF, rt; (b) 2 M BH₃-SMe₂ in THF; (c) **6**, EDC, HOBt, DMF.

Table 1

In vitro TRPV1 antagonistic activities for 2-alkylthio derivatives












R	K_i [CAP] (nM)	IC_{50} [pH] (nM)	R	K_i [CAP] (nM)	IC_{50} [pH] (nM)
1	28	1281	14 	WE	WE
2	0.2	6.3	15 	27.4	1498
7	0.7	40.4	16 	3.3	312
8	2.5	95.6	17 	3.0	250
9	5.6	719	18 	2.9	217
10	0.7	82	19 	WE	WE
11	4.3	WE	20 	WE	WE
12	7	68	21 	48.2	1099
13	2.3	118	22 	85	WE

Table 2

In vitro TRPV1 antagonistic activities for 2-cycloalkylthio derivatives

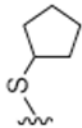
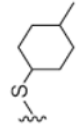
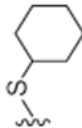
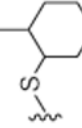
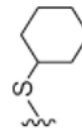
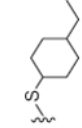
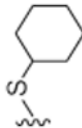
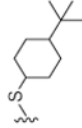
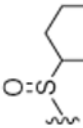
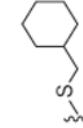
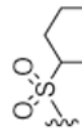
R	K_i [CAP] (nM)	IC ₅₀ [pH] (nM)	R	K_i [CAP] (nM)	IC ₅₀ [pH] (nM)
	1.2	WE		0.5	180
	0.9	WE		1.9	NE
	0.4	WE		1.0	WE
	43.5	WE		2.6	89.6
	WE	NE		2.3	254
	WE	NE			

Table 3

In vitro TRPV1 antagonistic activities for 2-arylmethylthio derivatives

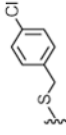
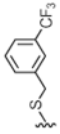
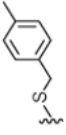
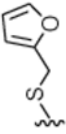
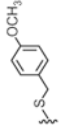
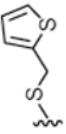
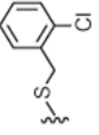
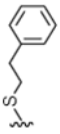
R	K_i [CAP] (nM)	IC ₅₀ [pH] (nM)	R	K_i [CAP] (nM)	IC ₅₀ [pH] (nM)
	8.7	674		3.9	71
	3.2	764		14.6	WE
	2.3	279		15	WE
	4.9	620		1.9	111

Table 4In vitro hTRPV1 antagonistic activities for **2** and **24S** to multiple activators

Activators, parameter	2	24S
CAP (f)K _i (nM)	0.2	0.4
NADA (f)K _i (nM)	0.01	0.05
pH, IC ₅₀ (nM)	6.3	>1000
Heat 45 °C, IC ₅₀ (nM)	0.8	22.3

Author Manuscript

Author Manuscript

Author Manuscript

Author Manuscript